

Superconducting density of states and vortex lattice of LaRu_2P_2 observed by Scanning Tunneling Spectroscopy

Marta Fernández-Lomana,^{1,2} Paula Obladen Aguilera,^{1,2} Beilun Wu,^{1,2}
Edwin Herrera,^{1,2} Hermann Suderow,^{1,2} and Isabel Guillamón^{1,2}

¹*Laboratorio de Bajas Temperaturas y Altos Campos Magnéticos,*

Departamento de Física de la Materia Condensada,

Instituto Nicolás Cabrera and Unidad Asociada UAM-CSIC,

Universidad Autónoma de Madrid, E-28049, Madrid, Spain

²*Condensed Matter Physics Center (IFIMAC), Universidad Autónoma de Madrid, E-28049, Madrid, Spain*

(Dated: January 26, 2026)

We provide the superconducting density of states of the iron based superconductor LaRu_2P_2 ($T_c = 4.1$ K), measured using millikelvin Scanning Tunneling Microscopy. From the tunneling conductance, we extract a density of states which shows the opening of a s-wave single superconducting gap. The temperature dependence of the gap also follows BCS theory. Under magnetic fields, vortices present Caroli de Gennes Matricon states, although these are strongly broadened by defect scattering. From the vortex core size we obtain a superconducting coherence length of $\xi = 50$ nm, compatible with the value extracted from macroscopic H_{c2} measurements. We discuss the comparison between s-wave LaRu_2P_2 and pnictide unconventional multiple gap and strongly correlated Fe based superconductors.

LaRu_2P_2 ($T_c = 4.1$ K) was the pnictide superconductor with the highest T_c known before the discovery of high T_c superconductivity in non-stoichiometric pnictide superconductors [1–3].

High T_c superconductivity in the pnictides and iron based superconductors indeed often appears in doped compounds. A relevant and well examined example is the BaFe_2As_2 system, which is an antiferromagnet that becomes superconducting by doping with holes and with electrons [4, 5]. Isoelectronic compounds in its stoichiometric composition, such as BaRu_2As_2 or BaFe_2P_2 , do not exhibit superconductivity [6, 7].

LaRu_2P_2 is isoelectronic to LaFe_2As_2 . Both crystallize in the tetragonal ThCr_2Si_2 structure and have three dimensional Fermi surfaces. However, whereas LaRu_2P_2 is a superconductor with a T_c of 4.1 K, LaFe_2As_2 is not [8]. A similar case is found in the isoelectronic oxyde compounds LaRuPO and LaFePO . These materials show similar Fermi surfaces with strong 2D character. LaRuPO is non-superconducting whereas LaFePO is superconducting with a T_c of 6 K [9]. The substitution of Fe-3d orbitals with the much less localized Ru-4d orbitals leads to an increased bandwidth, resulting in reduced electronic correlations and lower values of the effective mass [10, 11]. However, in the compounds with 3D electronic properties, LaRu_2P_2 and LaFe_2As_2 , superconductivity is found in the material with smaller electronic correlations suggesting that the origin of superconductivity in LaRu_2P_2 is different than in other pnictide superconductors [8].

LaRu_2P_2 presents under pressure a transition to a collapsed tetragonal phase in which the c-axis lattice parameter decreases by as much as 10% [12]. The collapsed tetragonal phase arises at low pressures in systems with large steric effects, such as CaFe_2As_2 [13]. The steric effects are partially lifted in $\text{CaKFe}_4\text{As}_4$ and in KFe_2As_2 compounds, which also show a transition to the col-

lapsed tetragonal phase under pressure. Superconductivity remains with a higher T_c in the collapsed tetragonal phase of KFe_2As_2 [14] and is suppressed in the collapsed tetragonal phases of $\text{CaKFe}_4\text{As}_4$ [15] and CaFe_2As_2 [16]. LaRu_2P_2 under external pressure presents a collapsed tetragonal phase above 2 GPa which is not superconducting [17, 18].

Band structure calculations, Angular Resolved Photoemission (ARPES), and de Haas van Alphen measurements all show that the electronic band structure of LaRu_2P_2 is very different than the one found in many other pnictide superconductors [3, 8]. The Fermi surface has a strong three-dimensional character and consists of two sets of sheets derived from the Ru-4d orbitals that form a donut with a small hole centered around the Z point, a warped electron cylinder at the corners of the Brillouin zone, and an additional open three-dimensional sheet derived from a combination of La and Ru-4d orbitals [3, 8]. The tubes at the corners of the Brillouin zone are the only zones of the Fermi surface that can be considered close to two-dimensional; the rest of the Fermi surface is largely three-dimensional. Mass renormalization is practically absent over the whole band structure, suggesting that superconductivity in LaRu_2P_2 is not related to electronic correlations but rather to electron-phonon coupling [1, 19].

To better understand the role played by electron-phonon interactions it is fundamental to know the superconducting gap structure of LaRu_2P_2 . Here we provide microscopic measurements of the superconducting gap of LaRu_2P_2 using Scanning Tunneling Microscopy (STM). We find a highly isotropic gap and study the vortex phase. We find that the superconducting coherence length is much larger than the coherence length of other iron pnictide superconductors. Our data establish LaRu_2P_2 as a nearly isotropic s-wave superconductor, contrasting anisotropic correlated electron superconduc-

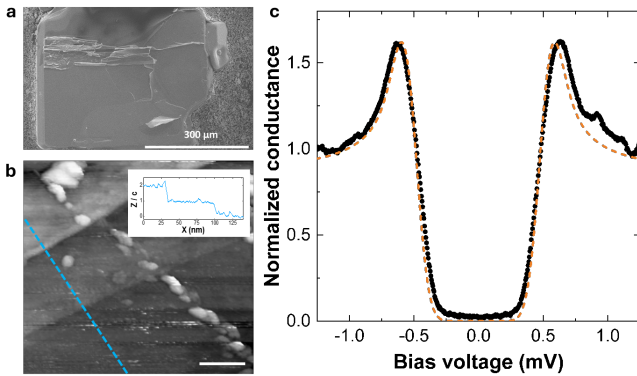


FIG. 1. a) Scanning Electron Microscope (SEM) image of a LaRu₂P₂ sample after cryogenic cleaving and after removing the sample from the STM. b) STM image of the topography of the sample, taken with a bias voltage $V=2.5$ mV, a constant tunneling current $I_t=2$ nA and at $T=80$ mK. In the inset we show the profile normalized to the c-axis lattice parameter of LaRu₂P₂, taken along the blue line. White scale bar is 40 nm long. c) Normalized conductance as a function of bias voltage measured at 80 mK (black) and a fit to the BCS theory (dashed line), with $\Delta=0.61$ meV.

tivity found in other pnictide superconducting materials.

To perform the STM study of LaRu₂P₂, we cleaved up to five single crystalline samples at 4 K and under cryogenic vacuum conditions (see a picture of a sample in Fig. 1a). Samples were grown using flux growth [22], as described in Ref. [23]. It has been very difficult to obtain flat surfaces in LaRu₂P₂, in spite of searching more than thirty different fields of view using the in-situ positioning mechanism described in Ref. [24]. Being a three-dimensional crystal, the cleaving procedure might be complex and strain-free homogeneous surfaces might be difficult to create. Here we focus on the few particular surfaces where we found flat terraces and neat superconducting features. In Fig. 1b, steps with a height of one unit cell can be seen. We use a STM described in Ref. [25] and the software described in Refs. [26, 27]. The resolution in energy is below 8 μeV and the lowest temperatures of our set-up is below 100 mK, as shown in Ref. [25].

Fig. 1c presents the measured conductance on one of these surfaces at 80 mK and 0 T. The conductance shows the opening of a superconducting gap with zero density of states at zero bias and well developed quasi-particle peaks. We have fitted our data using BCS expression (orange dashed line in Fig. 1c) and obtain $\Delta=0.61$ meV which is $\Delta=1.72k_BT_c$ for $T_c=4.1$ K. This is in agreement with the T_c obtained by macroscopic measurements [1, 3, 8, 19].

In Fig. 2a we show the normalized conductance as a function of bias voltage for different temperatures ranging from 84 mK to 3 K. Solid colored lines provide the convolution of the density of states with the derivative of the Fermi function. In Fig. 2b we show the density of

states used for the convolution at each temperature, as described in Refs. [20, 25, 28–32]. The size of the energy gap is given by the position of the peaks in the density of states. The gap as a function of temperature is shown in Fig. 2c. The dashed line is the temperature dependence of the gap within BCS theory. We can see that the temperature dependence of the gap size extracted from the experiment follows well BCS theory.

Fig. 3a and b show conductance maps at 0 mV for magnetic fields of 0.05 T and 0.07 T (approximately 0.43 H_{c2} and 0.61 H_{c2} , with $H_{c2}=0.127$ T [23]). In the 0.05 T map we observe a few vortices. We see that vortices do not form an ordered triangular lattice, possibly due to the large intervortex separation and due to pinning. Nevertheless, the average intervortex distance is 213 ± 50 nm, which is compatible with the distance expected from Abrikosov theory for a triangular vortex lattice at 0.05 T, which is 215 nm.

In Fig. 3c we show the normalized conductance curves outside and inside the vortex core. Outside the vortex core, we observe the usual superconducting gap. At the centre of the vortex core, the superconducting gap vanishes and we observe instead a broad peak in the tunneling conductance centred at zero bias.

Due to multiple Andreev scattering and the singular shape of the order parameter at the vortex core, quantized states can form inside vortices, particularly, when the ratio Δ^2/E_F is large. These states are called Caroli de Gennes Matricon (CdGM) states [33]. LaRu₂P₂ does not present correlations, for which E_F is relatively large (0.58 eV). As Δ is relatively small (0.61 meV), Δ^2/E_F is small in LaRu₂P₂. In such a situation, CdGM vortex cores states are averaged into a single sharp peak at the vortex core, as observed for instance in 2H-NbSe₂ [29, 34–36]. Contrary to 2H-NbSe₂ and related systems, in LaRu₂P₂, the electronic mean free path $\ell \leq \xi$, so that the peak is strongly broadened by impurity scattering [20, 29, 36].

To quantify the size of the vortex core in LaRu₂P₂, we followed the method described in Ref. [21, 37]. In Fig. 3d we show the radially averaged and normalized tunneling conductance around two vortices at 0.05 T and 0.07 T. From these profiles, we extract the vortex core size and plot it against the magnetic field in Fig. 3e. We normalize the magnetic field to H_{c2} and compare the same quantity for other superconducting compounds [32]. The vortices in LaRu₂P₂ are by more than an order of magnitude larger than the vortices in other materials. From the extrapolation of the vortex core size to H_{c2} we obtain for the superconducting coherence length $\xi \simeq 52$ nm. This value is in good agreement with the value of ξ obtained through macroscopic measurements ($\xi \approx 50$ nm, see Ref. [18]).

Thus, our results show that LaRu₂P₂ is a s-wave BCS superconductor with a low critical field and a large coherence length. Vortices present localized CdGM states, in agreement with s-wave superconductivity. Likely, it is a phonon-mediated superconductor with a rather isotropic

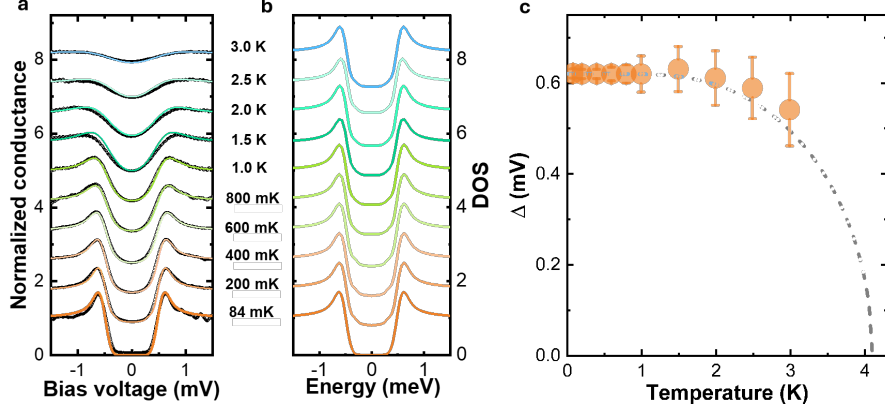


FIG. 2. **a)** The normalized conductance as a function of bias voltage measured from 84 mK to 3 K is shown as black data points. The solid colored lines represent the convoluted density of states (DOS) with their respective temperatures. **b)** The DOS obtained from the curves in a) is plotted as a function of energy from 84 mK to 3 K. **c)** The temperature dependence of the superconducting gap is determined by the quasiparticle peak position of the DOS.

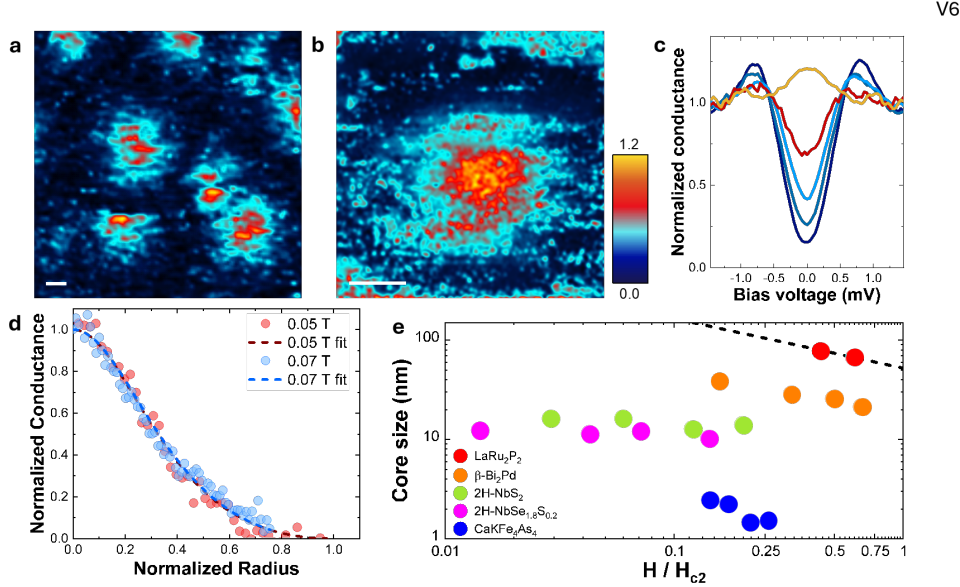


FIG. 3. **a),b)** Zero bias tunneling conductance maps made at magnetic fields 0.05 T and 0.07 T respectively. Images are taken at different locations at 90 mK. White scale bar: 50 nm. The bar at the left provides the color scale in units of the normalized conductance. Vortex positions are Delaunay triangulated. **c)** Normalized conductance along a line from inside to outside of a vortex. The conductance curves follow the same color code as the conductance map in a) and b). **d)** Normalized conductance vs distance from vortex centre normalized as [20], at different magnetic fields. **e)** Vortex core size vs the magnetic field in LaRu₂P₂ compared to the core size in other superconductors (β -Bi₂Pd, 2H-NbS₂, 2H-NbSe_{1.8}S_{0.2} [20] and CaKFe₄As₄ [20]). Dashed line shows the fit $C = \eta\sqrt{\Phi_0/\pi H}$, described in the text [21].

superconducting gap structure.

The Eliashberg spectral function has been obtained for LaRu₂P₂ in Ref. [38]. The Eliashberg spectral function describes the probability distribution of phonon frequencies and the strength of their coupling with electrons. The T_c calculated in Ref. [38] is very close to the actual observed T_c . The phonon structure in LaRu₂P₂ shows

two soft modes out of the a-b plane. The electron phonon coupling for these soft modes is particularly large because of their coupling to the Ru-4d orbitals, presenting a high electronic density of states [38]. These modes might soften further under pressure and be related to the collapsed tetragonal transition observed above 2 GPa, which renders LaRu₂P₂ non superconducting [17, 18].

Often, well defined directional soft modes produce anisotropic gap structures and are observed in the tunneling spectroscopy [39]. The Ru-4d character is spread out over the Fermi surface, which eliminates anisotropies, and probably favors a homogeneous superconducting gap. As we show here, the superconducting gap of LaRu₂P₂ is rather isotropic over the Fermi surface, suggesting that electron-phonon coupling is also isotropic. All this makes it very difficult to identify phonon modes the tunneling spectroscopy.

On the other hand, LaRu₂P₂ lacks a two-dimensional hole pocket at the center of the Brillouin zone [3, 8]. The multiple values of the superconducting gap often found in Fe based materials [20, 40] are related to the set of two-dimensional pockets and the coexistence with other order such as antiferromagnetism (AFM) with wavevectors that connect the pockets at the centre and at the borders of the Brillouin zone. Our results suggest that the interactions among these two sets of bands are crucial to create conditions favouring superconductivity with largely different superconducting gap values. This suggests, in turn, that multiple gap, high critical temperature and s⁺⁻ superconductivity in the Fe based pnictides arise from electronic interactions between different bands crossing the Fermi level.

In summary, we have determined the superconducting

density of states and observed vortices in LaRu₂P₂ using STM. We find that there are no states at the Fermi level and no signatures for a large distribution of values of the superconducting gap. The gap follows the temperature dependence expected from s-wave BCS theory. From the vortex core size, we determine the coherence length ($\xi \approx 50$ nm). Our measurements show that the microscopic properties of LaRu₂P₂ are very similar to those of electron-phonon mediated intermetallic superconductors.

ACKNOWLEDGMENTS

This work was supported by the Spanish Research State Agency (PID2020-114071RB-I00, CEX2023-001316-M, TED2021-130546B-I00), by the Comunidad de Madrid through program NANOMAGCOST-CM (Program No.S2018/NMT-4321) and by the European Research Council PNICTEYES grant agreement 679080 and by VectorFieldImaging grant agreement 101069239. We acknowledge collaborations through EU program Cost CA21144 (Superqumap). We acknowledge segain-vev for the support in cryogenics and for the design and construction of STM equipment. We also thank Rafael Álvarez Montoya and José María Castilla for technical support.

[1] W. Jeitschko, R. Glaum, and L. Boonk, Superconducting LaRu₂P₂ and other alkaline earth and rare earth metal ruthenium and osmium phosphides and arsenides with ThCr₂Si₂ structure , Journal of solid state chemistry **69**, 93 (1987).

[2] Y. Kamihara, T. Watanabe, M. Hirano, and H. Hosono, Iron-based layered superconductor La[O_{1-x} F_x]FeAs (x= 0.05–0.12) with T_c =26 K, Journal of the American Chemical Society **130**, 3296 (2008).

[3] E. Razzoli, M. Kobayashi, V. Strocov, B. Delley, Z. Bukowski, J. Karpinski, N. Plumb, M. Radovic, J. Chang, and T. Schmittetal, Bulk electronic structure of superconducting LaRu₂P₂ single crystals measured by soft-x-ray angle-resolved photoemission spectroscopy, Phys. Rev. Lett. **108**, 257005 (2012).

[4] M. Rotter, M. Tegel, and D. Johrendt, Superconductivity at 38 K in the Iron Arsenide Ba_{1-x}K_xFe₂As₂, Phys. Rev. Lett. **101**, 107006 (2008).

[5] A. S. Sefat, R. Jin, M. A. McGuire, B. C. Sales, D. J. Singh, and D. Mandrus, Superconductivity at 22 K in Co-Doped BaFe₂As₂, Phys. Rev. Lett. **101**, 117004 (2008).

[6] S. Sharma, A. Bharathi, S. Chandra, V. R. Reddy, S. Paulraj, A. T. Satya, V. S. Sastry, A. Gupta, and C. S. Sundar, Superconductivity in Ru-substituted polycrystalline Ba(Fe_{1-x}Ru_x)₂As₂ , Phys. Rev. B **81**, 174512 (2010).

[7] S. Jiang, H. Xing, G. Xuan, C. Wang, Z. Ren, C. Feng, J. Dai, Z. Xu, and G. Cao, Superconductivity up to 30 K in the vicinity of the quantum critical point in BaFe₂(As_{1-x}P_x), Journal of Physics: Condensed Matter **21**, 382203 (2009).

[8] P.J.Moll, J. Kanter, R. McDonald, F. Balakirev, P. Blaha, K. Schwarz, Z. Bukowski, N.D.Zhigadlo, S. Karych, and K. Mattenbergeretal, Quantum oscillations of the superconductor LaRu₂P₂: Comparable mass enhancement 1 in Ru and Fe phosphides , Phys. Rev. B **84**, 224507 (2011).

[9] J. J. Hamlin, R. E. Baumbach, D. A. Zocco, T. A. Sayles, and M. B. Maple, Superconductivity in single crystals of LaFePO, Journal of Physics: Condensed Matter **20**, 365220 (2008).

[10] V. Brouet, F. Rullier-Albenque, M. Marsi, B. Mansart, M. Aichhorn, S. Biermann, J. Faure, L. Perfetti, A. Taleb-Ibrahimi, and P. LeFet, Significant reduction of electronic correlations upon isovalent Ru substitution of BaFe₂As₂ , Phys. Rev. Lett. **105**, 087001 (2010).

[11] H. Muranaka, Y. Doi, K. Katayama, H. Sugawara, R. Settai, F. Honda, T. D. Matsuda, Y. Haga, H. Yamagami, and Y. Ōnuki, Two-Dimensional Fermi Surfaces in LaRuPO and LaFePO versus Three-Dimensional Fermi Surfaces in LaFe₂P₂, Journal of the Physical Society of Japan **78**, 053705 (2009).

[12] G. Drachuck, A. Sapkota, W. Jayasekara, K. Kothapalli, S. Bud'ko, A. Goldman, A. Kreyssig, and P. Canfield, Collapsed tetragonal phase transition in LaRu₂P₂ , Phys. Rev. B **96**, 184509 (2017).

[13] M. S. Torikachvili, S. L. Bud'ko, N. Ni, and P. C. Canfield, Pressure Induced Superconductivity in CaFe₂As₂, Phys. Rev. Lett. **101**, 057006 (2008).

[14] Y. Nakajima, R. Wang, T. Metz, X. Wang, L. Wang, H. Cynn, S. T. Weir, J. R. Jeffries, and J. Paglione, High-temperature superconductivity stabilized by electron-

hole interband coupling in collapsed tetragonal phase of KFe_2As_2 under high pressure, *Phys. Rev. B* **91**, 060508 (2015).

[15] U. S. Kaluarachchi, V. Taufour, A. Sapkota, V. Borisov, T. Kong, W. R. Meier, K. Kothapalli, B. G. Ueland, A. Kreyssig, R. Valentí, R. J. McQueeney, A. I. Goldman, S. L. Bud'ko, and P. C. Canfield, Pressure-induced half-collapsed-tetragonal phase in $\text{CaKFe}_4\text{As}_4$, *Phys. Rev. B* **96**, 140501 (2017).

[16] A. van Roekeghem, P. Richard, X. Shi, S. Wu, L. Zeng, B. Saparov, Y. Ohtsubo, T. Qian, A. S. Sefat, S. Biermann, and H. Ding, Tetragonal and collapsed-tetragonal phases of CaFe_2As_2 : A view from angle-resolved photoemission and dynamical mean-field theory, *Phys. Rev. B* **93**, 245139 (2016).

[17] N. Foroozani, J. Lim, J. Schilling, R. Fotovat, C. Zheng, and R. Hoffmann, Hydrostatic high-pressure studies to 25 GPa on the model superconducting pnictide LaRu_2P_2 , *Journal of Physics: Conference Series* Vol. **500**, 032007 (2014).

[18] B. Li, P. Lu, J. Liu, J. Sun, S. Li, X. Zhu, and H.-H. Wen, Pressure induced enhancement of superconductivity in LaRu_2P_2 , *Scientific reports* **6**, 24479 (2016).

[19] J. Ying, Y. Yan, R. Liu, X. Wang, A. Wang, M. Zhang, Z. Xiang, and X. Chen, Isotropic superconductivity in LaRu_2P_2 with the ThCr_2Si_2 -type structure, *Superconductor Science and Technology* **23**, 115009 (2010).

[20] A. Fente, W. R. Meier, T. Kong, V. G. Kogan, S. L. Bud'ko, P. C. Canfield, I. Guillamón, and H. Suderow, Influence of multiband sign-changing superconductivity on vortex cores and vortex pinning in stoichiometric high- T_c $\text{CaKFe}_4\text{As}_4$, *Phys. Rev. B* **97**, 134501 (2018).

[21] A. Fente, E. Herrera, I. Guillamón, H. Suderow, S. Mañas Valero, M. Galbiati, E. Coronado, and V. G. Kogan, Field dependence of the vortex core size probed by scanning tunneling microscopy, *Phys. Rev. B* **94**, 014517 (2016).

[22] P. C. Canfield and I. R. Fisher, High-temperature solution growth of intermetallic single crystals and quasicrystals, *Journal of Crystal Growth* **225**, 155 (2001), proceedings of the 12th American Conference on Crystal Growth and Epitaxy.

[23] M. Fernández-Lomana, V. Barrena, B. Wu, S. Delgado, F. Mompeán, M. García-Hernández, H. Suderow, and I. Guillamón, Large magnetoresistance in the iron-free pnictide superconductor LaRu_2P_2 , *Journal of Physics: Condensed Matter* **33**, 145501 (2021).

[24] H. Suderow, I. Guillamón, and S. Vieira, Compact very low temperature scanning tunneling microscope with mechanically driven horizontal linear positioning stage, *Review of Scientific Instruments* **82**, 033711 (2011).

[25] M. Fernández-Lomana, B. Wu, F. Martín-Vega, R. Sánchez-Barquilla, R. Álvarez Montoya, J. M. Castilla, J. Navarrete, J. R. Marijuan, E. Herrera, H. Suderow, and I. Guillamón, Millikelvin scanning tunneling microscope at 20/22 T with a graphite enabled stick-slip approach and an energy resolution below 8 μeV : Application to conductance quantization at 20 T in single atom point contacts of Al and Au and to the charge density wave of 2H-NbSe₂, *Review of Scientific Instruments* **92**, 093701 (2021).

[26] F. Martín-Vega, V. Barrena, R. Sánchez-Barquilla, M. Fernández-Lomana, J. B. Llorens, B. Wu, A. Fente, D. P. Duplain, I. Horcas, R. López, J. Blanco, J. A. Higuera, S. Mañas-Valero, N. H. Jo, J. Schmidt, P. C. Canfield, G. Rubio-Bollinger, J. G. Rodrigo, E. Herrera, I. Guillamón, and H. Suderow, Simplified feedback control system for scanning tunneling microscopy, *Review of Scientific Instruments* **92**, 103705 (2021).

[27] I. Horcas, R. Fernández, J. M. Gómez-Rodríguez, J. Colchero, J. Gómez-Herrero, and A. M. Baro, WSXM: A software for scanning probe microscopy and a tool for nanotechnology, *Review of Scientific Instruments* **78**, 013705 (2007).

[28] H. Suderow, Superconducting density of states from scanning tunneling microscopy, in *Encyclopedia of Condensed Matter Physics (Second Edition)*, edited by T. Chakraborty (Academic Press, Oxford, 2024) second edition ed., pp. 600–615.

[29] I. Guillamón, H. Suderow, S. Vieira, L. Cario, P. Diener, and P. Rodiere, Superconducting density of states and vortex cores of 2H-NbS₂, *Phys. Rev. Lett.* **101**, 166407 (2008).

[30] E. Herrera, B. Wu, E. O'Leary, A. M. Ruiz, M. Águeda, P. G. Talavera, V. Barrena, J. Azpeitia, C. Munuera, M. García-Hernández, L.-L. Wang, A. Kaminski, P. C. Canfield, J. J. Baldoví, I. Guillamón, and H. Suderow, Band structure, superconductivity, and polytypism in AuSn_4 , *Phys. Rev. Mater.* **7**, 024804 (2023).

[31] F. Martín-Vega, E. Herrera, B. Wu, V. Barrena, F. J. Mompeán, M. García-Hernández, P. C. Canfield, A. M. Black-Schaffer, J. J. Baldoví, I. Guillamón, and H. Suderow, Superconducting density of states and band structure at the surface of the candidate topological superconductor Au_2Pb , *Phys. Rev. Res.* **4**, 023241 (2022).

[32] E. Herrera, I. Guillamón, J. A. Galvis, A. Correa, A. Fente, R. F. Luccas, F. J. Mompeán, M. García-Hernández, S. Vieira, J. P. Brison, and H. Suderow, Magnetic field dependence of the density of states in the multiband superconductor $\beta - \text{Bi}_2\text{Pd}$, *Phys. Rev. B* **92**, 054507 (2015).

[33] C. Caroli, P. G. de Gennes, and J. Matricon, Bound states on a vortex line in a type II superconductor, *Phys. Letters* **9**, 10.1016/0031-9163(64)90375-0 (1964).

[34] H. F. Hess, R. B. Robinson, and J. V. Waszczak, Vortex-core structure observed with a scanning tunneling microscope, *Phys. Rev. Lett.* **64**, 2711 (1990).

[35] H. F. Hess, R. B. Robinson, R. C. Dynes, J. M. Valles, and J. V. Waszczak, Scanning-Tunneling-Microscope Observation of the Abrikosov Flux Lattice and the Density of States near and inside a Fluxoid, *Phys. Rev. Lett.* **62**, 214 (1989).

[36] N. Hayashi, T. Isoshima, M. Ichioka, and K. Machida, Low-Lying Quasiparticle Excitations around a Vortex Core in Quantum Limit, *Phys. Rev. Lett.* **80**, 2921 (1998).

[37] V. G. Kogan and N. V. Zhelezina, Field dependence of the vortex core size, *Phys. Rev. B* **71**, 134505 (2005).

[38] E. Karaca, S. K. g, H.M.T, G. Srivastava, and S. U. gur, First-principles investigation of superconductivity in the body-centred tetragonal, *Philosophical Magazine* **96**, 2059 (2016).

[39] H. Suderow, P. Martínez-Samper, N. Luchier, J. P. Brison, S. Vieira, and P. C. Canfield, Tunneling spectroscopy in the magnetic superconductor $\text{TmNi}_2\text{B}_2\text{C}$, *Phys. Rev. B* **64**, 020503 (2001).

[40] P. O. Sprau, A. Kostin, A. Kreisel, A. E. Böhmer, V. Taufour, P. C. Canfield, S. Mukherjee, P. J. Hirschfeld, B. M. Andersen, and J. C. S. Davis, Discovery of orbital-selective Cooper pairing in FeSe, *Science* **357**, 75 (2017).